

## STRENGTH AND STIFFNESS ASSESSMENT TECHNOLOGIES FOR IMPROVING GRADING EFFECTIVENESS OF RADIATA PINE WOOD

Henri Baillères,<sup>a,\*</sup> Gary Hopewell,<sup>a</sup> Geoff Boughton,<sup>b</sup> and Loic Brancheriau<sup>c</sup>

This work was designed to provide the Australian structural radiata pine processing industry with some indications for improving stress grading methods and/or technologies to give an increase in structural grade yields, and significantly reduce processing costs without compromising product quality. To achieve this, advanced statistical techniques were used in conjunction with state-of-the-art property measurement systems applied to the same sample of sawn timber. Acoustic vibration analyses were conducted on green and dry boards. Raw data from existing in-line systems was captured on the same boards. The Metriguard HCLT stress rating system was used as the “reference” machine grading because of its current common use in the industry. A WoodEye® optical scanning system and an X-ray LHG scanner were also able to provide relevant information on knots. The data set was analyzed using classical and advanced statistical tools to provide correlations between data sets, and to develop efficient strength and stiffness prediction equations. Reductions in non-structural dry volumes can be achieved.

*Keywords:* Modulus of elasticity; Modulus of rupture; Grading; Knot; Stress rating; Resonance method; X-ray

*Contact information:* a: Agri-Science Queensland, Department of Employment, Economic Development and Innovation, 50 Evans Rd, Salisbury, 4107 QLD, Australia; b: TimberED Services Pty. Ltd., Po Box 30 Duncraig East, WA 6023, Australia; c: CIRAD - PERSYST Department, Research unit: Production and Processing of Tropical Woods, TA B-40/16, 73 Rue Jean François Breton, 34398 Montpellier, France; \*Corresponding author: henri.bailleres@deedi.qld.gov.au

### INTRODUCTION

The use of timber in load bearing applications in building construction requires the estimation of the mechanical properties of each structural wooden member. Because of its natural variability, timber used for structural purposes has to be graded according to relevant mechanical properties, such as strength or stiffness. In Australia, the design properties for pine specified in the Australian Standard AS 1720.1 (1997) were based on several large national in-grade testing programs. The characteristic values were then determined based on nationally pooled data from these tests and using the calculation procedure in AS/NZS 4063 (1992). A suite of stress grades used for machine-graded softwoods in Australia was defined (Bolden *et al.* 1994) and later refined (Boughton and Juniper 2010). In the Australian industry, this grading is performed through widely used automatic systems. Machine strength grading of sawn timber is based on correlations between grade indicating properties and measured physical properties (AS/NZS 1748,

1997). When new types of machines are implemented, they are calibrated with timber samples representing the wood material which the machine will grade.

Stiffness is the easiest characteristic to estimate since it can be non-destructively measured directly by different techniques like machine stress rating or acoustic devices. The measured stiffness has to be calibrated against the standard reference stiffness, e.g. four point static bending (AS/NZS 4063 1992). The discrepancy always observed is understandable through the dissimilarity of the measurement methods, static versus dynamic, local versus global, and different modes of loading. Strength is more problematic to estimate as it cannot be measured directly, except in a destructive test, and it is mainly related to local phenomena.

Improved confidence in estimating strength and stiffness values for green and dried timber enables grading closer to design values, thus improving structural grade volumetric recoveries in sawn boards, resulting in a more efficient and profitable use of the resource. In comparing grading methods, the most relevant correlation is between the grading parameter and the strength measured from a specimen taken from the most strength-impairing physical feature along the length. The most effective methods have higher correlation coefficients as they are most able to correctly classify timber on the basis of strength.

Published results about the ability of different non-destructively measurable parameters applied to the same sample of sawn timber to predict timber bending strength using in-line grading equipment are based on few wide scope investigations (Hanhijärvi et al. 2005 and 2008; Blackmore et al. 2010). In some cases, the purpose of all these investigations has not necessarily included the establishment of relationships between non-destructive parameters and mechanical properties.

During Combigrade Phase 1, Hanhijärvi et al. (2005) reviewed the results from five previous investigations into non-destructive testing for strength prediction published between 1984 and 1997. Based on this review the following conclusions were drawn. The degree of success in accounting for variations (coefficient of determination,  $R^2$ ) varied between studies, probably due to differing materials and methods. The highest coefficient of determination relative to bending strength by any parameter tested achieved  $R^2=0.7$ . The modulus of elasticity (MOE) is the best single variable for prediction of strength (modulus of rupture, MOR), followed by the knot area ratio (KAR), and density. The prediction capability ( $R^2$  value) can be improved if two parameters are used together as predictors.

Other relevant findings were reported in the literature. Görlacher (1984) found that the natural frequency (dynamic MOE) correlated well with static test results, as did Blass and Gard (1994) in their tests on Douglas fir. In separate studies Sandoz (1989) and Diebold et al. (2000) found  $R^2=0.45$  and  $0.53$  respectively for ultrasonic speed and strength. On a small number of specimens Oja et al. (2000) found a prediction of  $R^2=0.41$  for X-ray (density and knot volume) and strength of sawn boards. Halabe et al. (1995) showed that the green stress wave velocity or the corresponding green MOE can directly be used to predict the dry static bending MOE.

Combigrade project phase 1 and 2 (Hanhijärvi et al. 2005 and 2008) included research on the potential of strength grading of dry timber with combined measurement techniques (X-ray, gamma ray, acoustic vibration, ultrasound, stress rating, and optical

assessment). The measure of the ability of a method to predict the grade determining properties is solely based on simple linear regression analysis through the coefficient of determination. Findings from the Combigrade project Phase 1 and 2 are summarized in the following conclusions. Spruce and pine populations behave differently in regard to the predictors, with stronger correlation between predictors and strength usually achieved by pine. Stiffness parameters gave the best single-variable predictions of bending strength with MOE measured by either static method, vibration method, or by ultrasonic method. X-ray scanning of boards achieved similar coefficients of determination to MOE measurements. Based on  $R^2$  values, knot parameters provide good predictions of strength and density for pine, but not for spruce. Irradiation equipment (X-ray and gamma ray) provides slightly better strength prediction than visual surface inspection method such as KAR. Sloping grain measurements did not have the potential to predict strength. Combinations of devices provided correlations with reference MOR of  $R^2=0.80$  to  $0.85$  for pine and  $0.60$  to  $0.65$  for spruce. Combination of knot measurements with density and annual ring width provides effective predictions for strength with  $R^2=0.7$  (pine) and  $0.6$  (spruce). Based on their results, the authors concluded that the best single parameter predictors of bending strength are the stiffness related parameters measured by either static method, vibration method or by ultrasonic method. However, X-ray scanning of boards (with several measured quantities) as a single measurement reaches the same level. As single methods for predicting strength, these can reach  $R^2$  values of  $0.5$  to  $0.6$  for spruce and  $0.7$  to  $0.75$  for pine. It is difficult to improve dramatically their  $R^2$  values with auxiliary measurements. However, combining stiffness parameters with knot or density measurements or X-ray measurement with stiffness parameters does improve the result enough to be profitable.

Brancheriau and Baillères (2003) performed acoustic tests on low-grade structural boards of larch (*Larix europaea*). Direct use of acoustic response spectra as predictive variables to estimate MOE and MOR in both edgewise and longitudinal vibration is the unique feature of the method. Estimates of MOE values were also computed using eigenfrequencies of the vibrating objects. Partial Least Squares (PLS) analysis of acoustic signals showed that the strength could be accurately estimated. The estimation was appreciably better than results obtained by linear regression with dynamic MOE.

These results, performed using various species, prove the potential of prediction improvement when a suitable analytical approach is developed. Conservatism in grading due to the lack of confidence in estimating stiffness and bending strength values for dried timber graded using traditional methods represents a huge loss for the pine processing industry in Australia. Improving structural grade yields results in a more efficient and profitable use of the Australian plantation softwood resource. The objective of this paper was to provide a basis for improved green and dry grading of Australian radiata pine to allow increased structural grade yields and reduced processing costs. The aim was to study the potential of different non-destructive methods that can be applied in-line to predict strength and stiffness of green and dry sawn boards. The potential of increasing prediction accuracy with combined methods was assessed. To achieve this, advanced statistical techniques were used in conjunction with state-of-the-art property measurement systems.

## EXPERIMENTAL

### Materials

The full study used material from three separate softwood resources in Australia (Baillères et al. 2009), but this paper will focus on only one.

Twenty-seven logs with an average centre diameter of 420 mm (range 300 mm to 580 mm) representing the strength-limited radiata pine (*Pinus radiata*) resource of Western Australia were provided for testing. The strength-limited radiata pine represented material with a low strength to stiffness ratio, and the 27 logs were selected from a resource known to produce this material. From all of the timber produced by these 27 logs only 429 boards were selected at random for the project. They were drawn at random from the production line. A deliberate decision was made to cut only one size (100 x 38 mm) from the log to prevent any bias due to the fact that larger pieces are cut from specific parts of the log. By cutting only one cross section, there was no bias to specific types of fibre in the sample; therefore the cutting pattern could not introduce an accidental bias of the results.

### Methods

In Australia normal in-grade testing for evaluation of characteristic properties values uses random-position tests (AS/NZS 4063). A random test is where the central position of the test span is allocated using a random number generator to determine the measurement datum along the board without consideration of any properties or features of the timber in allocating test position. A biased test involves selection of a particular feature or position on the piece and deliberate placement in the centre of the test span in order to focus the results on the feature selected. For edge-biased bending tests, the selected feature is placed on the tension edge. The random test is specified for determining characteristic values. However, grading requirements in Australia still require the grade of an individual piece to be related to the performance of the weakest point on the piece. Hence in testing the effectiveness of the grading operation, it is valid and necessary to compare the properties of the weakest (grade determining) location on the piece with the relevant grading parameters. The use of biased position testing to compare timber properties with grading parameters is consistent with grading qualification testing in AS/NZS 1748.2:2011.

In commercial grading, the verification testing by some producers normally use random-position tests and the test results feed back to the threshold settings to ensure that the design characteristic values are reliably obtained by each graded product. For this study, most use was made of the biased position test data. Successful grading methods will have a high correlation with the strength measured through a biased test. Although it is possible to achieve meaningful results from random-position tests, very large sample sizes are required to ensure that there are enough “weak points” tested to truly evaluate the grading method. The scatter of the results is generally high, as the test span may not contain any of the limiting material that actually determined the grade of the piece (Leicester et al 1998).

Logs provided for the trials were selected from a mix of butt logs (30%) and top logs (70%) in order to focus the sample on timber normally expected to have a low

strength-to-stiffness ratio and ensure sufficient representation of low values of MOR. Each log was sawn into 100 x 38 mm sizes.

After completion of vibration tests in the green (unseasoned) condition, boards were transported to a commercial softwood plant for sawing and high temperature kiln drying to a target moisture content of 12%. After stabilization the test materials were dressed to 90 x 35 mm, a standard structural cross-sectional dimension used in the Australian building sector. The final length of the boards varied between 2.41 m to 5.05 m.

The trial flow is given below:

1. Vibration tests on green and dry boards
2. Machine stress rating of dry boards
3. X-Ray scanning of dry boards
4. Optical scanning of dry boards
5. Standard static bending test of dry boards

#### *Vibration tests*

The acoustic vibration measurements were captured using Bing® products (CIRAD, <http://www.xylo-metry.org/en/software.html>) software. The technique is also known as the resonance method, as it takes into account the resonance frequencies of a beam from its response to an impact. Bing® allows determination of the bending and compression MOE by analysis of the natural vibration spectrum of a piece of wood (dynamic MOE). Shear modulus and internal friction can also be assessed on beams of various cross section shapes (Brancheriau and Baillères 2003).

#### *Machine stress rating*

Metriguard 7200 High Capacity Lumber Tester (HCLT) equipment was used to measure MOE profiles. The boards were bent flatwise by rollers downward and then upward. The bending force and the deflection in both bending sections were measured and local MOEs at intervals of 13.88 mm were automatically calculated. The average and the low point MOE were provided on the full length (excluding the leading and trailing 820 mm end sections of boards). The predictors used for the analysis were the average (HCLTavg), the minimum value (HCLTmin), and the value at the centre of the test span (HCLTtest) from the MOE profile.

#### *X-Ray scanning*

A Linear High Grader (LHG) uses X-Ray technology to analyze density variation allowing the identification of knots within boards. The LHG was developed by Coe Newnes/McGehee ULC (Canada). Two parameters were extracted from the X-Ray profile: LHGkar (estimation of knot area ratio) and LHGwkar (same as LHGkar with a specific weighted window).

### Optical scanning

A WoodEye® optical scanning system was used to record defect type, size, and location with a spatial resolution around 1 mm. The WoodEye® scanning system used combines: grey scale camera, colour camera, tracheid effect laser, and profile detection laser. The sensor-system scans each piece on all four sides for a wide range of natural features. Each is classified, for example a knot may be described as a black knot, sound knot, or fibre knot. Board geometry is also fully described in the output of the scan.

### Standard static bending tests

The specimens were conditioned to a temperature of  $20 \pm 3^\circ\text{C}$  and in an environment having a relative humidity of  $65 \pm 5\%$ . This conditioning was maintained until the moisture content was stable. Moisture content was checked using an electric resistance moisture meter to confirm that the boards had been conditioned to the range specified in the AS/NZS 4063 standard (10 - 15 %).

Four-point static bending tests were performed using a testing method in accordance with AS/NZS 4063:1992 (equivalent to European Standard test EN 408, March 2004). The load for the reference testing was applied and measured with a Shimadzu UDH-30 metric ton (300 kN) universal testing machine. The support consists of a solid steel roller 240 mm long by 50 mm diameter and a flat mounting plate. In the middle of the span the deflection was measured with a strain gauge type linear displacement transducer. The bending test span was 1620 mm with load applied at two points, and the span-to-depth ratio was 18:1. The load deflection curve was measured up to 1.6 kN for all specimens. The global MOE was determined from the slope of the linear relationship between the applied load ( $P$ ) and the resulting deflection ( $w$ ) using the following equation (AS/NZS4063, 1992),

$$MOE = \frac{23}{108} \cdot \frac{l_s^3}{bh^3} \cdot \frac{\Delta P}{\Delta w} \quad (1)$$

with  $b$ : width,  $h$ : height, and  $l_s$ : span. After removal of the displacement transducer, loading continued until failure of the specimen. MOR was calculated using the equation (2),

$$MOR = 18 \cdot \frac{P_{\max}}{bh} \quad (2)$$

with  $P_{\max}$ : maximum load.

The maximum error of measurement was calculated from the equation (1) and (2) by a calculus method using the maximum uncertainty of each sensor and expressed in the form of relative errors. The maximum error for static MOE was 11%, and it was 6% for MOR. Static tests were performed by placing the critical zone (maximum strength reducing defect) in the centre of the test span (European Standard EN 384, §5.2, March 2004). The location of the maximum strength reducing defect was manually assessed by an experienced testing officer.

*Specific data extraction*

Automated data extraction was undertaken to obtain specific non-destructive parameters associated with the optical scanning technique and the acoustic resonance technique. The optical profile construction is based on a discrete rendering process over the length of the beam in 1 cm steps. Each profile step is associated with a defects' projection in a measurement window with a length of two times the height of the beam. The projection window can be rectangular on the entire beam width, rectangular external; 1/3 of the top and bottom part of the beam height, rectangular interior; 1/3 of the centre part of the beam height, or a diamond-shaped pattern centred on the cross section. All the profiles are filtered with a Blackman sliding-window of which the size is equivalent to the beam height. Descriptions of the WoodEye® parameters are provided in Appendix 1. The vibration spectra (resonance technique) were analyzed in order to provide a range of vibration signal descriptors described in Appendix 2. The frequency range was 0 to 2000 Hz in longitudinal vibration (sampling frequency of 20000 Hz with a resolution of 1.2 Hz). The typical number of Eigenfrequencies analyzed was 3 in longitudinal vibration.

*Data analysis*

HCLT devices were considered as the “benchmark” grading machine because of their common use in industry. All statistical analysis methods were performed using the R software (version 2.9.1) with PLS library (Mevik and Wehrens 2007).

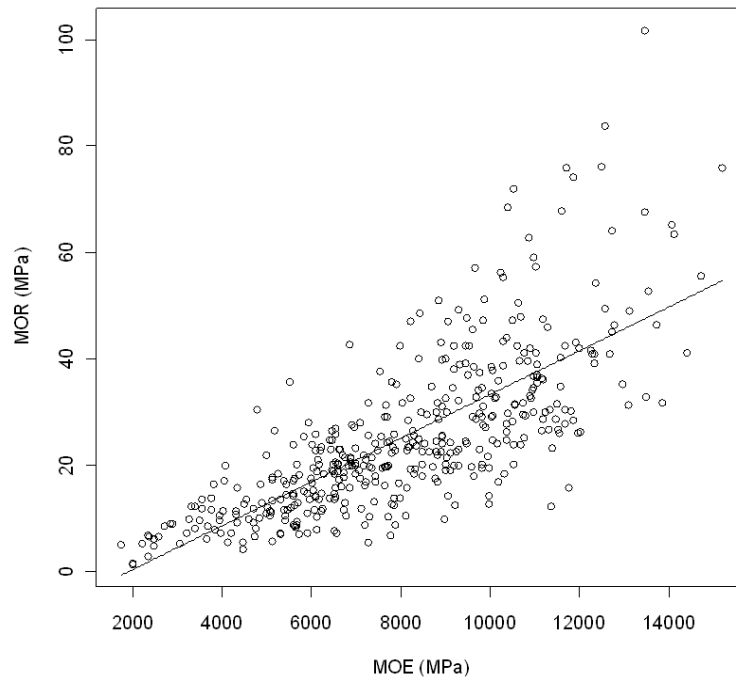
**RESULTS AND DISCUSSION****Static Bending**

Table 1 displays descriptive statistics for density, MOE, and MOR at a moisture content of 12% for all the boards tested (N = 429). MOR parameter had a high coefficient of variation (COV = 59%) with values ranging from less than 5 MPa to 100 MPa (1st quartile = 14 MPa and 3rd quartile = 32 MPa).

**Table 1.** Descriptive Statistics of Density and Static Properties (N=429)

Property	Mean	COV (%)
Density (kg/m <sup>3</sup> )	510	8
MOE (MPa)	8000	34
MOR (MPa)	25	59
COV: coefficient of variation		

The relationship between static MOE and MOR was significant with an *R*-square value of  $R^2 = 0.56$  (residual standard error = 10 MPa, F-statistic = 540, *p*-value < 0.001, Fig. 1). The general observation was the “trumpet like shape” of the data scatter points, in other words residual error on MOR increased with the MOE. This could induce a source of heteroscedasticity problems (non-homogeneous variances) when developing linear regression equations.



**Fig. 1.** Relationship between static MOE and MOR ( $R^2= 0.56$ ,  $N=429$ ).

**Analysis of Optical and Dynamic Parameters**

Figure 2 shows a histogram of optical defects recorded on the boards. The histogram was computed by counting the defects of the same type on all the boards, consequently the frequencies displayed are not an average per board; they are from all recorded defects.

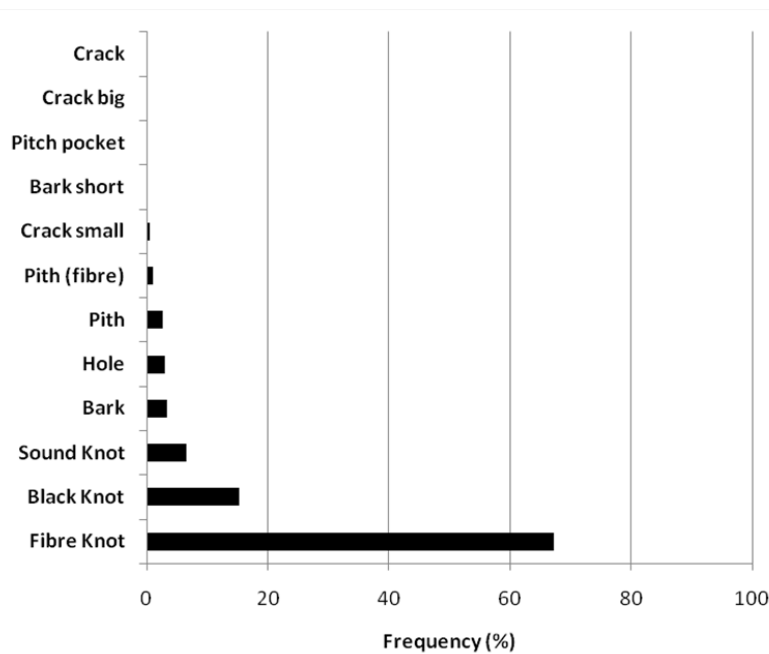


**Fig. 2.** Histogram of optical defects (color was not taken into account,  $N = 429$ ).

The knot categories were the most frequent (Fig. 2). Black knot and Sound knot categories referred to knot defects created from the grey scale cameras. The fibre knot category was created from the tracheid laser scattering sensor, which detects fibre disturbances. Therefore, often a given knot provides Fibre knot and Black or/and Sound knot information. The knot sizes returned for each knot type differed, even for the same knot in most of the cases due to the detection methods. Fibre knots tended to return larger size measurements than the other classifications. In analyzing the optical data output, only the size of a given knot was used, and its classification by colour or measurement technique was ignored. For each knot the total projected area covered by the envelope of all knot categories was computed.

For each defect two main parameters were computed along each board based on the raw optical data (Appendix 1): a material inertia ratio (CTR) and a pseudo knot area ratio (pKAR). All grading measurements were compared with the test MOR and MOE, so only the measurements that directly affected the MOR and MOE were used. A sensitivity study was used to determine the region of interest centred on the test span over which the grading measurements were combined. PLS, a specific multiple linear regression method (Brancheriau and Baillères 2003), was used with each predictor being a position along the span. MOR was the dependent variable. The values associated to predictors were the pKAR at the given position. The profiles contained 162 values (1.62 m span) which led to 162 predictors for the PLS procedure (N = 429).

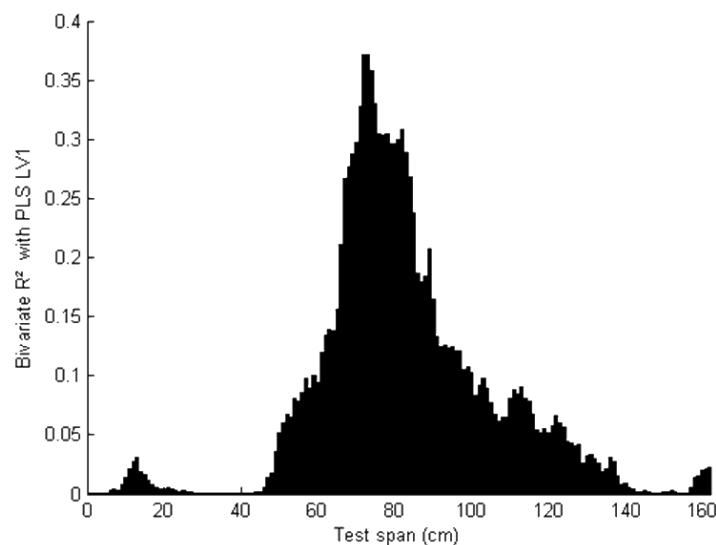


**Fig. 3.** Bivariate  $R^2$  between pKAR profiles and the first PLS component (LV1), dependent variable MOR (N = 429).

Only one PLS component was highly significant (8% of variance for the predictors and 31% of variance for MOR). Figure 3 displays the bivariate  $R^2$  coefficient between pKAR values along each profile and the first PLS component. It shows that pKAR values between the internal loading points had a significant contribution in the prediction of MOR (positions of loading points are 54 cm and 108 cm). It was thus not

necessary to compute pKAR parameters with profiles outside the internal loading points (dimension of the computation window of pKAR parameters).

Having established the appropriate region of interest for calculating the value of each parameter at the test location, the parameters could then be used to develop predictive algorithms. A principal component analysis (PCA) was used to study correlations among optical and 'dry' dynamic parameters by grouping these parameters into a few factors (Number of parameters = 29, N = 429, Table 2). The principal components were based on the correlation matrix computation followed by a Varimax rotation. The purpose of this rotation was to obtain interpretable orthogonal components (each parameter was associated with a minimal number of components). Table 2 presents the results of this analysis. The parameters are listed down the table and the components across the table.

Eight principal components were extracted (with an associated Eigenvalue over 0.95). These components represented 81% of variance of the original parameters. Table 2 shows that the component PC1 combined the pKAR associated parameters. The CTR parameters were linked with PC5 and PC8 with a difference between the mean value (PC5) and the 5% percentile (PC8). The 5% percentile was equivalent to the minimum value. MOE parameters were linked with PC4. Basic signal descriptors (SCG and SBW) and signal energy parameters were scattered between PC2, PC3, PC6, and PC7. SSP, MIF, Q1, Q2, Q3, and MPow1 were not highly correlated with one particular component. CTR, pKAR, and dynamic parameters contained independent information.

### Efficiency of Individual Predictors for Grading

Each of the grading parameters was tested for its correlation with reference static bending MOE and MOR obtained on dry boards. When considering grading parameters from green boards, the vibration MOE in compression acquired on green boards provides the best correlation with reference static bending MOE and MOR acquired on dry boards ( $R^2=0.58$  and  $R^2=0.25$  respectively).

When considering grading parameters from dry boards, the Metriguard HCLT provided the strongest correlation ( $R^2=0.70$ ) with static MOE, using the minimum MOE from the profile on the static bending test span (local measurement). The average MOE from Metriguard CLT and the dynamic MOE deliver comparable quality of prediction ( $R^2=0.64$  and  $R^2=0.65$  respectively). Interestingly, the specific MOE (MOE extracted from vibration measurement without density information) correlation was in the same magnitude of order to the best correlations, indicating that simple vibration (no density measurement) systems may form the basis of an effective pre-grading tool.

For MOR, the dynamic MOE provided  $R^2$  of 0.28. Three signal descriptors, the spectral centre of gravity ( $R^2=0.10$ ), the spectral slope ( $R^2=0.15$ ), and the spectral bandwidth ( $R^2=0.16$ ), provide a level of prediction significantly lower than the best optical scanner parameters ( $R^2$  between 0.30 and 0.40). WoodEye® pKAR provided the best coefficient of determination with MOR, surpassing LHG X-ray by 0.1 (0.36 vs 0.25 respectively). The Metriguard minimum MOE contains the majority of the information and combining with LHG only improves by a magnitude of 0.06.

**Table 2.** Bivariate Correlations Matrix (PCA with Varimax Rotation on Optical and Dynamic Parameters on Seasoned Boards, N=429)

Parameter	PC1	PC2	PC3	PC4	PC5	PC6	PC7	PC8
CTR_AC_M	-0.31	0.05	-0.07	0.22	<b>0.99</b>	-0.12	-0.07	-0.30
CTR_AC_5	-0.39	-0.03	-0.07	0.16	0.09	-0.16	-0.09	<b>-0.94</b>
CTR_trgl_AC_M	-0.31	0.04	-0.07	0.22	<b>0.99</b>	-0.13	-0.09	-0.31
CTR_trgl_AC_5	-0.62	0.04	-0.07	0.28	0.51	-0.19	-0.10	<b>-0.91</b>
pKAR_ext_M	<b>0.93</b>	-0.10	0.10	-0.26	-0.33	0.22	0.11	0.52
pKAR_ext_99	<b>0.89</b>	-0.09	0.05	-0.22	-0.27	0.19	0.05	0.55
pKAR_int_M	<b>0.89</b>	-0.05	0.09	-0.29	-0.29	0.17	0.13	0.36
pKAR_int_99	<b>0.83</b>	-0.05	0.01	-0.26	-0.22	0.10	0.06	0.30
pKAR_trgl_M	<b>0.96</b>	-0.09	0.10	-0.28	-0.35	0.23	0.13	0.49
pKAR_trgl_99	<b>0.96</b>	-0.09	0.05	-0.25	-0.30	0.19	0.07	0.51
SCG	0.14	<b>-0.93</b>	0.30	-0.42	-0.08	-0.14	-0.24	0.06
SBW	0.21	<b>-0.88</b>	0.06	-0.55	-0.11	-0.12	-0.19	0.08
SSP	0.11	-0.32	-0.44	-0.55	-0.07	-0.18	-0.22	0.04
MIF	0.03	-0.63	-0.22	0.15	-0.03	-0.06	-0.48	-0.07
MOE1	-0.28	0.46	-0.16	<b>0.93</b>	0.22	-0.12	-0.02	-0.16
Q1	-0.25	0.01	-0.30	0.44	0.15	-0.39	-0.06	0.00
NrjR1	-0.07	0.25	<b>-0.92</b>	0.21	0.07	-0.02	0.04	-0.06
Pow1	-0.11	0.08	-0.40	0.15	0.10	-0.70	-0.19	-0.14
SBNrjR1	-0.09	0.26	<b>-0.91</b>	0.19	0.06	-0.03	0.06	-0.06
MOE2	-0.24	0.41	-0.15	<b>0.93</b>	0.18	-0.08	-0.12	-0.17
Q2	-0.26	0.05	-0.24	0.50	0.12	-0.43	-0.57	-0.12
NrjR2	-0.08	0.02	<b>-0.77</b>	0.14	0.08	-0.16	-0.55	-0.11
Pow2	-0.10	-0.17	0.03	0.05	0.06	<b>-0.82</b>	-0.54	-0.14
SBNrjR2	-0.09	-0.20	0.03	0.03	0.05	-0.27	<b>-0.93</b>	-0.10
MOE3	-0.21	0.01	-0.24	<b>0.89</b>	0.21	-0.18	-0.24	-0.18
Q3	-0.19	-0.26	-0.20	0.38	0.10	-0.42	-0.31	-0.17
NrjR3	-0.02	-0.64	0.31	-0.04	0.07	-0.32	<b>-0.74</b>	-0.06
Pow3	-0.12	-0.54	0.40	-0.03	0.06	<b>-0.71</b>	-0.20	-0.07
SBNrjR3	-0.03	<b>-0.72</b>	0.53	-0.13	0.04	-0.26	-0.01	-0.05

Correlations below -0.70 and above +0.70 are displayed in bold

### Efficiency of Combined Parameters for Grading

PLS regression was applied to estimate the MOR with the optical and the dynamic “dry” parameters as predictors (Fig. 4). This modelling method was performed before using a multiple linear regression (MLR) in order to underline the different combinations of parameters, which could appropriately estimate MOR. The number of predictors was 29 with 429 observations. The significant level of correlations between the predictors (Table 2) leads to a collinearity issue, which thus excludes the use of MLR.

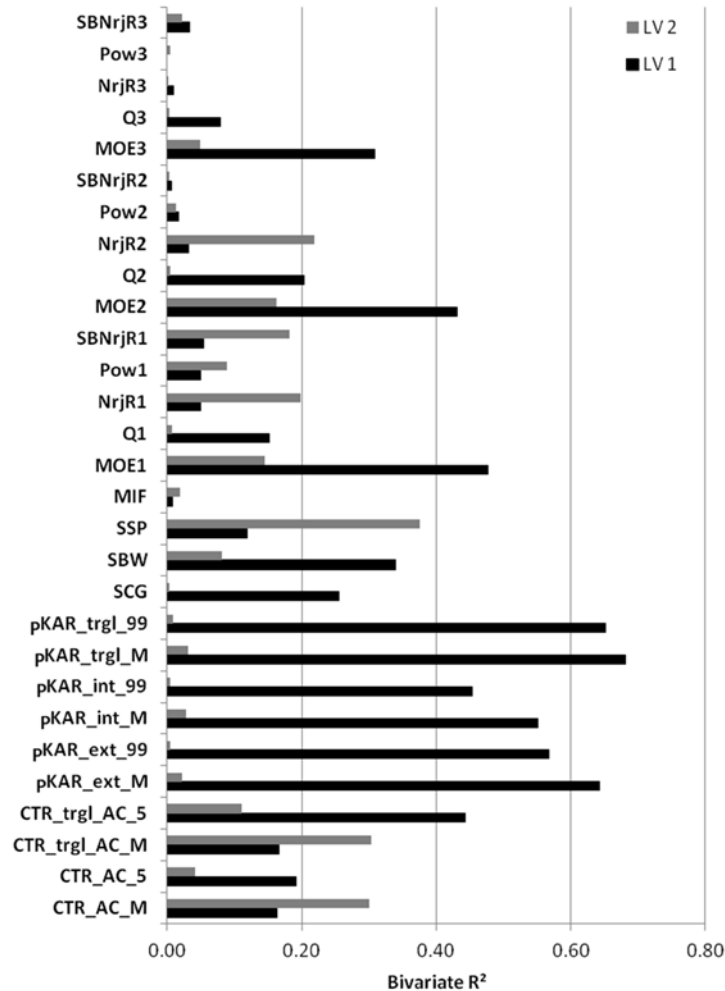


**Fig. 4.** Bivariate  $R^2$  coeff. between parameters and PLS components (MOR,  $R^2=0.49$ ,  $N=429$ )

For optimizing prediction of strength the coefficient of determination was  $R^2 = 0.49$  (residual standard error = 11 MPa, F-statistic = 206,  $p$ -value < 0.001). From the PLS analysis, one possible set of predictors was extracted when applying a simplification procedure (backward elimination method, for example). Two PLS components were extracted (LV1, LV2). The links between original predictors and components are shown in Fig. 4. pKAR parameters were shown to be the most linked with PLS LV1. Dynamic MOEs, one CTR parameter (CTR\_trgl\_AC\_5) and basic signal descriptors (SCG and SBW) were also included in LV1. The component LV2 was mainly constituted by 2 CTR

parameters (CTR\_AC\_M, CTR\_trgl\_AC\_M) and a basic signal descriptor (SSP). One can notice that a very few dynamic parameters were of importance here. A possible explanation of this phenomenon was that only a portion of each board was statically tested, whereas dynamic parameters provide overall information of the board. If all boards were of static bending span length (1.62 m), then dynamic parameters associated with the second longitudinal mode would certainly be much more correlated with PLS LVs because the associated antinode of vibration is located in the middle of the tested beam, which corresponds to most influential part for MOR (Fig. 3).

### Optimum Combination of Predictors for Grading

MLR with simplification procedure were used to extract the relevant parameters. The model simplification procedure was a forward selection using the Akaike's criterion (Crawley 2005). To deal with heteroscedasticity, a transformation was applied on the dependent variable. Many approaches are possible to deal with non-constant variance of residues: weighted least squares, mixed model, generalized linear models or transformation of the dependent variable (Faraway 2002). Weighted least squares and generalized linear models assume that the form of the variance is exactly known. However, it is a common procedure to transform the dependent variable by its square root or natural logarithm (Faraway 2002). The square root transformation was chosen in this study because the inverse transformation (squared) was less sensitive to measurement error than for an exponential transformation (the inverse of natural logarithm).

**Table 3.** Multiple Linear & Non-linear Modelling of the Strength Property (N=429)

Dependent	Parameters	Covariables and coefficients	R <sup>2</sup>	SEC	Residue
MOR	HCLT and LHG on dry boards	HCLTmin, LHGkar 0.0022, -29, 18	0.41	11.4	2.6
	Optical and dynamic on dry boards	pKAR_trgl_99, MOE1, Q1, SSP -0.31, 0.0019, 0.058, -0.049, 18	0.49	10.7	2.0
	Optical and dynamic on green boards	pKAR_trgl_99, MOE1 -0.33, 0.0027, 16	0.46	10.9	2.4
$\sqrt{\text{MOR}}$	Optical and dynamic on dry boards	pKAR_trgl_99, MOE1, Q1 -0.030, 0.00022, 0.0055, 3.5	0.51	10.5	1.0
	Optical and dynamic on green boards	pKAR_trgl_99, MOE1 -0.032, 0.00026, 3.9	0.48	10.7	1.0

SEC: standard error of calibration (residual standard error) in MPa  
Residue: number of boards with negative error divided by those with positive error  
The last coefficient is the constant of the model

Combining vibration measurements with local information obtained from WoodEye® or Metriguard, significantly improves dry MOE prediction ( $R^2$  from 0.68 up to 0.77). There is only marginal improvement by combining all three methods. The characteristic knotty nature of this resource heavily impacts the MOE from random tests. Combining local parameters with global measurements resulted in a significant improvement in the prediction. Table 3 shows the results obtained in estimating MOR with dry or green boards. The first observation was that the results were equivalent between the combinations: optical with dynamic and HCLT with LHG. For both combinations the standard error of calibration was equal to 11 MPa for the linear modelling.

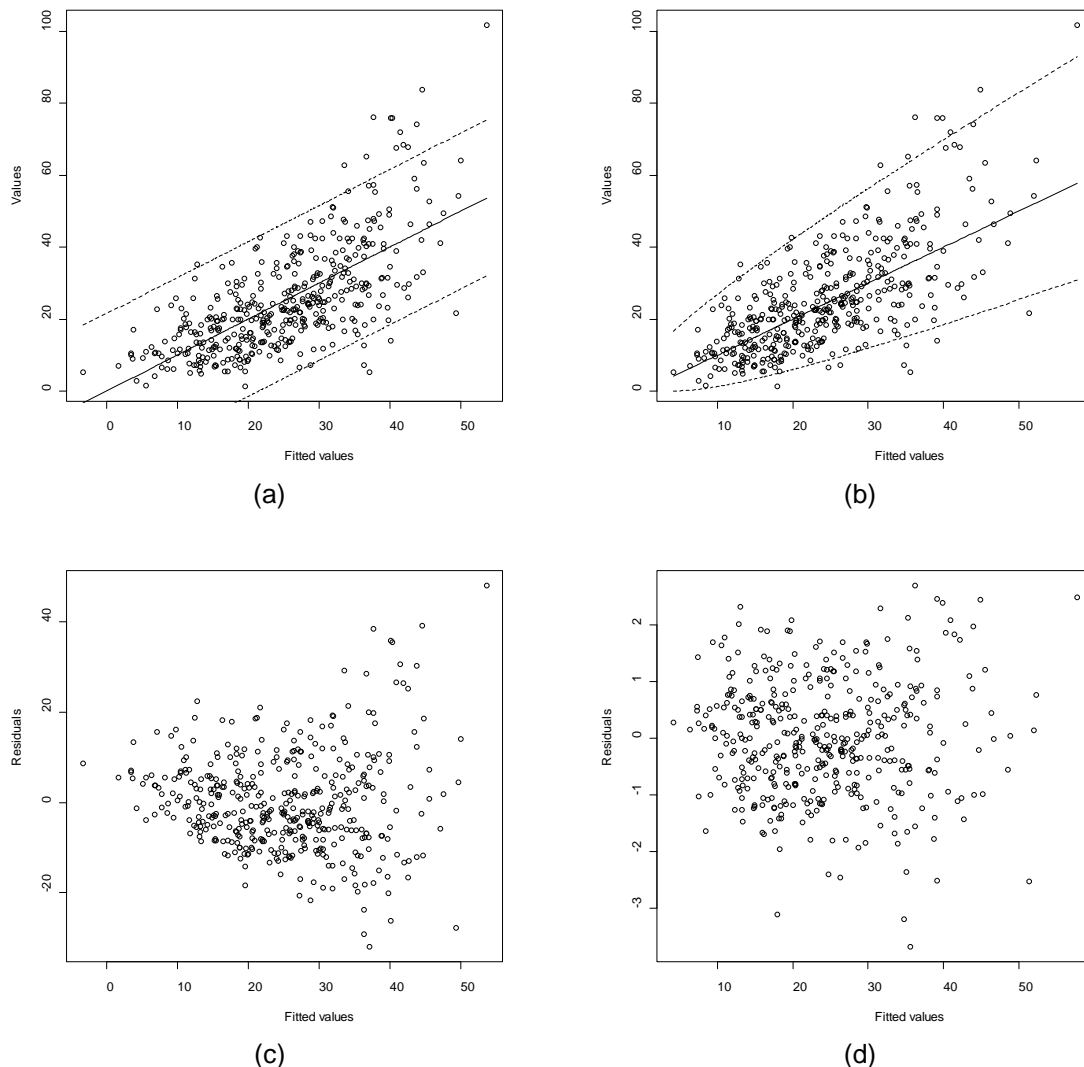


**Fig. 5.** (a) Relationship between MOR and optical-dynamic parameters on green boards ( $R^2=0.46$ ,  $N=429$ ); (b) Non-linear modelling between MOR and optical-dynamic parameters on green boards ( $R^2=0.48$ ,  $N=429$ ); (c) Residual plot associated with the linear model; (d) Residual plot associated with the nonlinear model

Few parameters were extracted; mostly the pKAR parameter (pKAR\_trgl\_99 equivalent to the maximum pKAR) and the MOE1 parameter (dynamic modulus associated with the fundamental frequency). Dynamic signal parameters (Q1 and SSP) were of less importance and were related with the energy loss during the dynamic motion. The plots show heteroscedasticity (Fig. 5-c) associated with an imbalance between over-estimation and under-estimation for low MOR (Residue ratio between 2.0 to 2.6, Table 3). Linear models of Table 3 overestimated the MOR (Figs. 5-a and 5-c). This phenomenon was corrected by taking the square root of MOR values (Residue ratio equal to unity in Table 3, Figs. 5-b and 5-d).

Alternative models were also tested without taking into account the pKAR parameters and the dynamic MOEs (square root of MOR as dependent variable, results

not shown in Table 3). The results were (1) five predictors were included in the models for dry or green boards; (2) the  $R^2$  values varied from 0.38 for dry boards to 0.30 for green boards; (3) the main parameters in the models were CTR\_trgl\_AC\_5, SSP, SBW, and quality factors (Q). The signal parameters were influenced by the moisture content of the boards which explained the drop of  $R^2$  values. These parameters were descriptors of the spectrum shape (SSP and SBW) or descriptors of the shape of each individual mode (Q). Viscoelastic behaviour and the presence of defects had an influence on these parameters.

## CONCLUSIONS

1. On dry boards of the strength-limited radiata pine wood resource, Metriguard HCLT, provides a better strength prediction due to this equipment's ability to measure mechanical local characteristics. The combination of grading equipment specifically for stiffness related predictors (Metriguard or vibration) with defect detection systems (optical or X-ray scanner) provides a higher level of prediction, especially for MOR.
2. For MOR assessment, the results were equivalent between the combinations: optical with dynamic and HCLT with LHG. For both combinations, the standard error of calibration was equal to 11 MPa for the linear modelling.
3. For the combination optical scanner and acoustic device, pKAR parameters, MOE, and dynamic signal parameters related with the energy loss during the dynamic motion provided a higher level of correlation than the reference machine grading used in this work.
4. The ability to provide an initial grading on green boards can increase significantly the profitability of the mill by saving the cost of drying and subsequent processing for non-structural grade boards sold at the same price whether green or dry. Reductions in non-structural dry volumes can be achieved by differing combinations of equipment, and their strategic location within the processing chain. As an example, in this study a combination of optical scanner and vibration measurements devices located on the green processing chain could significantly improve the MOR prediction even when compared to more conventional equipment like HCLT and LHG located on the dry processing chain. This approach should improve the efficiency of the mill. The improvement will vary depending of the wood resource.
5. The results of this work indicate a good potential for grading in the green mill, ahead of kiln drying and subsequent processes.

## ACKNOWLEDGMENTS

This work is a part of the project "MOE and MOR assessment technologies for improving graded recovery of exotic pines in Australia" (Baillères et al. 2009). The successful conduct of this work was made possible through the enthusiastic support from management and staff of the following organizations: Wespine, Bunbury Western Australia; Hyne Timber, Tumbarumba New South Wales, and Tuan Queensland,

Australia; Carter Holt Harvey, Myrtleford Victoria and Caboolture (formerly Weyerhaeuser) Queensland, Australia; Queensland Primary Industries and Fisheries, Brisbane Queensland, Australia; CIRAD Xylometry, Montpellier, France.

## REFERENCES CITED

- AS/NZS 4063 (1992). "Characterization of structural timber, Parts 1 & 2," Standards Australia and Standards New Zealand, Sydney and Wellington.
- AS/NZS 1748.1 (1997). "Timber – Stress-graded – Product requirements for mechanically stress graded timber," Standards Australia and Standards New Zealand, Sydney and Wellington.
- AS/NZS 1748.2 (2011). "Timber - Solid - Stress-graded for structural purposes - Qualification of grading method," Standards Australia and Standards New Zealand, Sydney and Wellington.
- AS 1720.1. (1997). "Timber structures, Part 1: Design methods," Standards Australia, Sydney.
- AS/NZS 4490. (1997). "Timber-Stress-graded-Procedure for monitoring structural properties," Standards Australia and Standards New Zealand, Sydney and Wellington.
- Baillères, H., Hopewell, G., and Boughton G. (2009). "MOE and MOR assessment technologies for improving graded recovery of exotic pines in Australia," Forest and Wood Products Australia Limited, Research Report PNB040-0708. Available at: <<http://www.fwpa.com.au/MOE-and-MOR-assessment-technologies-for-improving-graded-recovery-of-exotic-pines-in-Australia>> (accessed 20.12.11).
- Blakemore, P., Cown, D., Dumbrell, I., McKinley, R., Lyon, A., Barr, B., and Northway, R. (2010). "Western Australian Softwood Resource Evaluation: a survey of key characteristics of the *Pinus radiata* and *Pinus pinaster* resources in Western Australia with links to product performance of trees sampled from each resource, as determined by a processing study," Forest and Wood Products Australia Limited, Project No. PNC059-0809. Available at: <<http://www.fwpa.com.au/node/174>> (accessed 20.12.11).
- Blass, H., and Gard, W. (1994). "Machine strength grading of timber," Pacific Timber Engineering Conference, Australia, 598-603.
- Bolden, S. A., Leicester, R. H., Walsh, P. F., Young, F.G, Grant, D. J, and Seath, C. A. (1994). "In-grade evaluation of Australian pine –Structural properties of mechanically stress graded Australian pine," Pacific Timber Engineering Conference, Australia, 1994.
- Boughton, G. N., and Juniper, P. M. (2010). "Revision of Australian MGP stress grades 2009," in Proceedings World Conference on Timber Engineering 2010, Riva del Garda, Italy.
- Brancheriau, L., and Baillères, H. (2003). "Use of the partial least squares method with acoustic vibration spectra as a new grading technique for structural timber," *Holzforschung* 57(6), 644-652.
- Crawley, M. J. (2005). *Statistics: An Introduction using R*, ed., Wiley.

- Diebold, R., Schleifer, A., and Glos, P. (2000). "Machine grading of structural sawn timber from various softwood and hardwood species," *12th International Symposium on Non-destructive Testing of Wood*, Hungary, 139-146.
- EN 408:2003-08. (\_\_\_\_). "Timber structures – Structural timber and glued laminated timber – Determination of some physical and mechanical properties," CEN European Committee for Standardization.
- EN 384:2004-01. (\_\_\_\_). "Structural timber – Determination of characteristic values of mechanical properties and density," CEN European Committee for Standardization.
- Faraway, J. J. (2002). *Practical Regression and ANOVA Using R*, online book (<http://cran.r-project.org/doc/contrib/Faraway-PRA.pdf>) (accessed 20.12.11).
- Görlacher, R. (1984). "Ein neues Messverfahren zur Bestimmung des Elastizitätsmoduls von Holz," *Holz als Roh- und Werkstoff* 42, 219-222.
- Halabe, U. B., Bidigalu, G. M., GangaRao, H. V. S., and Ross, R. J. (1995). "Nondestructive evaluation of green wood using stress wave and transverse vibration techniques," *Materials Evaluation* 55(9), 1013-1018.
- Hanhijärvi, A., and Ranta-Maunus, A. (2008). "Development of strength grading of timber using combined measurement techniques," Report of the Combigrade project - phase 2. VTT Publications (<http://www.vtt.fi>) (accessed 20.12.11).
- Hanhijärvi, A., Ranta-Maunus, A., and Turk, G. (2005). "Potential of strength grading of timber with combined measurement techniques," Report of the Combigrade project - phase 1. VTT Publications (<http://www.vtt.fi>) (accessed 20.12.11).
- Leicester, R. H., Breitingner, H., and Fordham, H. (1998). "A comparison of in-grade test procedures," Proceedings of the CIB-W18B Meeting on Timber Structures. Savonlinna, Finland: Paper no. 31-5-2, 14 pages.
- Mevik, B. H., and Wehrens, R. (2007). "The PLS package: Principal component and partial least squares regression in R," *Journal of Statistical Software* 18(2), 1-24.
- Oja, J., Grundberg, S., and Grönlund, A. (2000). "Predicting the strength of sawn products by X-ray scanning of logs: A preliminary study," *Wood and Fiber Science* 32, 203-208.
- Sandoz, J. L. (1989). "Grading of construction timber by ultrasound," *Wood Science and Technology* 23, 95-108.

**APPENDIX 1: WoodEye® profile descriptions**

CTR	Material inertia ratio = calculated inertia / beam inertia ( $b \cdot h^3/12$ ). The inertia is calculated from the sum of inertias according to Parallel Axis Theorem (also known as Huygens-Steiner theorem). Profile is calculated between the internal loading points. Profile is weighted by the bending moment (unit maximum moment). Profile is equal to the product of the profiles from the 2 beam sides (noted A and C, sides related to the height).
CTR_AC_M	Rectangular window, mean value.
CTR_AC_5	5% percentile (equivalent to a minimum).
CTR_trgl_AC_M	Triangular window, mean value.
CTR_trgl_AC_5	5% percentile.
pKAR	Perimeter ratio = calculated perimeter / beam perimeter ( $2 \cdot (b+h)$ ). The perimeter is associated to defect height (sum of the heights). Profile is calculated between the internal loading points. Profile is equal to the sum of the profiles from the 4 beam sides.
pKAR_ext_M	1/3 external height for A and C, rectangular window, mean value.
pKAR_ext_99	99% percentile (equivalent to a maximum).
pKAR_int_M	1/3 internal height for A and C, rectangular window, mean value.
pKAR_int_99	99% percentile.
pKAR_trgl_M	Triangular window for A and C, mean value.
pKAR_trgl_99	99% percentile.

**APPENDIX 2: Dynamic parameter descriptions**

Dynamic MOE associated with the frequency ( $f_i$ ) in longitudinal vibration:

$$MOE_i = \rho \cdot \left( \frac{2 \cdot L \cdot f_i}{i} \right)^2, \quad i \in \{1, 2, 3\} \quad (3)$$

With  $L$ : length,  $\rho$ : density.

Spectral centre of gravity divided by the fundamental frequency ( $f_1$ ) in %:

$$SCG = \frac{1}{f_1} \sum_p A_p \cdot f_p / \sum_p A_p \quad (4)$$

With  $A_p$ : magnitude of the Discrete Fourier Transform.

Spectral bandwidth divided by the fundamental frequency ( $f_1$ ) in %:

$$SBW = \frac{1}{f_1} \sqrt{\frac{\sum_p A_p \cdot (f_p - SCG)^2}{\sum_p A_p}} \quad (5)$$

Spectral slope divided the fundamental frequency ( $f_1$ ) in %:

$$SSP = \frac{1}{f_1} \sqrt[3]{\frac{\sum_p A_p \cdot (f_p - SCG)^3}{\sum_p A_p}} \quad (6)$$

Quality factor (inverse internal friction) associated with the eigenfrequency of rank  $i$ :

$$Qi = \frac{\pi \cdot f_i}{\alpha_i} \quad (7)$$

With  $\alpha_i$ : temporal damping associated to  $f_i$ .

Modified inharmonicity factor in %:

$$MIF = \frac{f_2 \cdot f_3}{f_1^2} \quad (8)$$

Sub-band energy ratio (between the eigenfrequencies of rank  $i$  and  $j$ ):

$$NrjRi = \frac{\sum_{p=i}^j A_p^2}{\sum_{p=0}^{\text{Max}(p)} A_p^2} \quad (9)$$

Mean power of the sub-band defined by a pass band of -20dB centered on the eigenfrequency of rank  $i$ :

$$MPowi = \frac{\Delta f}{f_{\text{BandMax}} - f_{\text{BandMin}}} \sum_{p_{\text{BandMin}}}^{p_{\text{BandMax}}} A_p^2 \quad (10)$$

Sub-band energy ratio defined by a pass band of -20dB centered on the eigenfrequency of rank  $i$ :

$$SBNrjRi = \frac{\sum_{p_{\text{BandMin}}}^{p_{\text{BandMax}}} A_p^2}{\sum_{p=0}^{\text{Max}(p)} A_p^2} \quad (11)$$

Article submitted: October 18, 2011; Peer review completed: December 8, 2011; Revised version received and accepted: January 24, 2012; Published: January 27, 2012.